This paper is a non-peer reviewed preprint submitted to EarthArXiv.

This paper has been submitted to *Oceans*

Impact of the easternmost category-5 Hurricane Lorenzo on North Atlantic sea surface temperature and chlorophyll-a concentrations

Sérgio Muacho [1,2,*], Manoa Postec [3] and André Valente [4]

[1] Instituto Português do Mar e da Atmosfera, Divisão Oceanografia e Ambiente, 1495-165 Algés, Portugal; sergio.muacho@ipma.pt
[2] Centro de Ciências do Mar (CCMAR), Universidade do Algarve, Campus de Gambelas, 8005-139 Faro, Portugal.
[3] École nationale supérieure de techniques avancées Bretagne, 29200 Brest, France.
[4] Atlantic International Research Centre (AIR Centre), Parque de Ciência e Tecnologia da Ilha Terceira (TERI-NOV), 9700-702, Angra do Heroísmo, Portugal.
* Correspondence

Abstract

Hurricane Lorenzo was the easternmost Category 5 Atlantic hurricane on record. The impact of this exceptional storm on North Atlantic sea surface temperature and chlorophyll-a concentrations is investigated in this study using high-resolution daily interpolated satellite and model-derived datasets. Results show that Lorenzo induced strong sea surface cooling up to –2.5 °C and a significant increase in chlorophyll-a from 100 up to 250% relative to pre-storm conditions. Impacts were observed over a ~200 km-wide band along the right-hand side of the track and persisted for more than 10 days. Chlorophyll-a from different phytoplankton functional types were also examined. All major groups showed increased chlorophyll-a levels. Prokaryotes and Haptophytes dominated across the region both before and after the storm, though their relative dominance shifted at higher latitudes (35–40°N), where Haptophytes surpassed Prokaryotes as the leading community. Results highlight the distinctive imprint of this anomalous hurricane on the upper ocean, provide insights into alterations in phytoplankton communities and enable future comparisons for extreme atmospheric events in subtropical to midlatitude ocean.

Introduction

Tropical cyclone (TC) is the generic term for a rapidly rotating low-pressure weather system over tropical or subtropical waters. In the Atlantic, when a TC reaches maximum sustained winds of at least 119 km/h it is defined as a hurricane [1]. In general, TC and hurricane activity in the Atlantic occur from July to November, and major hurricanes form in the Main Development Region, defined as the tropical North Atlantic south of 21°N and the Caribbean Sea [2]. The Saffir-Simpson scale classifies hurricanes in terms of the intensity of their sustained winds, starting in Category 1 (119–153 km/h) and ending in Category 5 (≥252 km/h). Hagen and Landsea (2012) [3] reported 10 Category 5 hurricanes over the period 1992-2007; thus, approximately one every 1 to 2 years.

The extreme winds of TCs induce strong vertical mixing within the water column and have the capability to significantly alter the vertical thermal structure of the upper water column. Along their track, mixing leads to a cooling of the sea surface from 1 up to 4°C with most changes occurring along the right-hand side [4,5,6]. Price (2009) [7] refers 100 m as a typical depth of vertical mixing by a Category 3 hurricane. Through intense mixing, TCs impact biogeochemical processes through changes in the vertical distribution of phytoplankton and nutrients in the upper part of the water column.

Biological impacts of Atlantic TCs and hurricanes have been assessed with ocean color and infrared satellite imagery. Davis and Yan (2004) [8] and Babin et al. (2004) [9] demonstrated that TCs passage induced

decreases in sea surface temperature (SST), mixed layer deepening, and increases in surface chlorophyll-a concentration (CHL) in two different ocean environments as the northeast coast of the United States (eutrophic) and the Sargasso Sea (oligotrophic regime). Babin et al. (2004) [9] observed CHL enhancements of 5%-91%, persisting for 2–3 weeks after TCs, with stronger storms evidencing larger responses. The persistence and the lagged CHL response (few days) was consistent with nutrient-induced phytoplankton blooms, with additional contributions likely arising from mixing of the deep chlorophyll maximum (DCM). Walker et al. (2005) [10] also documented SST decreases and CHL increases along the TC track consistent with mixing of the DCM and enhanced growth from vertical inputs of nutrient-rich subsurface waters. Shropshire et al. (2016) [11] highlighted distinct responses to TCs in the Gulf of Mexico and the Sargasso Sea likely from contrasting depths of the DCM and the nutricline. Other regions beside the Atlantic are also affected by TCs. For instance, in the South China Sea, Zhao and Wang (2018) [12] investigated the impact of 74 TCs on CHL on a seasonal basis, while Li and Tang (2022) [13] found stronger CHL responses in the continental shelf (115%) compared to the open sea areas (57%).

Phytoplankton species exhibit distinct distribution patterns across the global ocean, driven by regional differences in nutrient availability, temperature, and light conditions [14,15,16]. They can be grouped into different Phytoplankton Functional Types (PFTs), such as diatoms, coccolithophores, cyanobacteria, and dinoflagellates, which differ in their ecological roles and biogeochemical functions, contributing differently to productivity, carbon export, and nutrient cycling [17]. Although the effects of TCs on CHL are well documented, few studies examined their impact on specific PFTs [18,19]. Avila-Alonso et al. (2023) [19] studied the impact of Hurricane Fabian (2003) based on a marine ecosystem model showing increases in all PFTs in the tropics (except for Prochlorococcus) associated with enhanced nutrient availability and limited zooplankton grazing. However, the model did not capture significant PFT perturbations in subtropical latitudes (north of 25°N). Mao et al. (2019) [18] also reported changes in phytoplankton assemblages following TC passages in the south China Sea based on water samples from cruise data, with dinoflagellates thriving while Bacillariophyta (diatoms) and Cyanophyta (prokaryotes) declined.

This study investigates the physical and biological impacts of Hurricane Lorenzo, the easternmost Category 5 Atlantic hurricane on record [20]. This uncommon storm formed from a tropical wave that moved off West Africa and developed into a Category 1 hurricane by 25 of September of 2019 (Figure 1). Subsequently, it rapidly intensified, reaching Category 5 hurricane strength on 29 September around 24°N, when the peak intensity was reported, with maximum 1-min sustained winds of 259 km/h and lowest pressure of 925 hPa [20]. Strong shear, dry air, and ocean cooling then weakened it to Category 2. Later on 2 of October moved west of Azores Archipelago (~38°N) as Category 1, where it resulted in the strongest local winds in 20 years [21]. Over its almost longitudinal course it affected the subtropical (~15°–35°N) and midlatitude (~ 35–45°N) North Atlantic. The affected subtropical area is generally characterized by low surface biomass relative to higher latitudes with persistently low surface CHL and a DCM below the euphotic zone [22, 23]. The northern midlatitude area presents higher mean surface CHL values and more pronounced spring blooms that play an important role in the Atlantic carbon pump [24]. The objective of this study is to evaluate the influence of the anomalous track of Hurricane Lorenzo on SST, CHL and PFTs, thereby providing insights into the role of this extreme storm in shaping regional physical and biogeochemical processes.

Data and Methods

This study relies on daily gap-free, high-resolution satellite-derived datasets to investigate upper-ocean responses to Hurricane Lorenzo. Specifically, we used datasets on sea surface temperature (SST), chlorophyll-a (CHL), and phytoplankton functional types (PFTs) to explore both the physical and biological dynamics associated with the storm. These datasets provide consistent spatial and temporal coverage to overcome the challenge of cloud cover in extreme weather conditions and help for a more robust characterization along and around the hurricane track.

Evaluation of SST changes relied on the daily gap-free L4 foundation SST data (i.e. free of diurnal variability; [25, 26]) from the Operational Sea Surface Temperature and Ice Analysis (OSTIA) system and

distributed by the Copernicus Marine Service (https://doi.org/10.48670/moi-00168). This data product combines observations from different satellite sources and techniques, including from infrared and microwave radiometry (ESA SST CCI, C3S, EUMETSAT OSI-SAF, and REMSS), as well as in situ SSTs from HadIOD providing gap-free SST maps at 0.05° x 0.05° horizontal grid resolution ([27], for details about the product).

For assessing CHL the daily L4 CHL data from the global multi-sensor GlobColour processor available from the Copernicus Marine Service were used (DOI. 10.48670/moi-00281). The Copernicus-GlobColour processor is a daily composite, with a 4 km x 4 km resolution, obtained by merging multiple ocean satellite sensor acquisitions (SeaWiFS, MODIS, MERIS, VIIRS-SNPP, JPSS1, OLCI-S3A, S3B) and by applying temporal averaging and interpolation methods to fill the missing data values ([28], for details about the product).

To assess the impact of Hurricane Lorenzo on SST and CHL daily anomalies were used. Daily SST and CHL anomalies were computed relative to the pre–hurricane SST and CHL conditions. Similar to other studies (e.g., Ruan et al., 2025 [29]), the mean SST and CHL concentration before the hurricane was defined as the average from the 5 days before the Lorenzo's passage (17–21 September). This approach allows the isolation of storm-induced signals and has been adopted in previous studies (e.g., Hanshaw et al. 2008 [30]). The use of anomalies also enables comparison across different regions, reducing bias due to latitudinal differences. Therefore, SST and CHL responses were calculated as the difference (for SST) and the ratio (for CHL) between the daily data and the 5-day average field before the storm.

For the PFTs, the Artificial Intelligence Global Daily (AIGD)-PFT dataset was used. The AIGD-PFT is a global, daily and gap-free dataset, with a spatial resolution of 4 km, providing estimates of the major phytoplankton functional types. The product was developed by combining artificial intelligence techniques through a Spatial–Temporal–Ecological Ensemble Deep Learning framework (STEE-DL) that integrates gap-filled ocean colour observations, physical and biogeochemical variables, and a global dataset of in situ HPLC pigment measurements to estimate chlorophyll-a concentrations for the major PFTs ([31], for more details). The IGD-PFT has been shown to produce accurate and temporally consistent PFT predictions and globally outperform other global daily PFT products (SynSenPFT, NOBM-daily) [31]. The dataset of this product was acquired from The National Tibetan Plateau/Third Pole Environment Data Center (https://doi.org/10.11888/RemoteSen.tpdc.301164).

To explore the responses of different phytoplankton communities to Hurricane Lorenzo passage, we analyzed PFTs separately by region instead of a spatial anomaly as with SST and CHL. Based on CHL and CHLA values, we defined three latitudinal bands of interest (15–25°N, 25–35°N, and 35–40°N) and the average values within each band (along Lorenzo's trajectory) were calculated as a function of time. The TC track was based on the data provided by the National Oceanic and Atmospheric Administration (NOAA) National Hurricane Center (data and details can be found at [20]).

Results

The storm Lorenzo was classified as a hurricane over an 8-day period (25 of September to 2 of October of 2009) across a broad region of the North Atlantic (13-43°N; Figure 1). To assess Lorenzo's impact on the upper ocean, we first computed the SST anomalies (SSTA) relative to the 5-day mean SST prior to the hurricane passage. Figure 2 shows the SSTA overlaid with Lorenzo's track and location at different hurricane stages and locations. These representative dates show the SSTA field after 2-, 7- and 11-days Lorenzo first entered the study area. In the last date, Lorenzo had moved north of the area of interest. The SSTAs reveal that Lorenzo produced basin-scale changes in thermal structure, with striking negative SSTA values along its path. Stronger negative anomalies up to - 2.5°C were found between 25°N and 37°N (Figures 2b and 2c), with relatively weaker response to the south and north of this latitudinal range, with anomalies of -1°C (Figure 2a). Additionally, the negative anomalies extend transversely over an approximately 2-3° longitude wide band along the cyclone's trajectory (~200-300 km, depending on latitude), with stronger negative values observed on the right-hand side of its track (Figures 2a, 2b and 2c). Overall, the colder signatures along the track remained for (at least) 10 days, as illustrated in Figure 2c for the region south of 25°N. The large-scale CHL distributions before, during, and after, the hurricane passage are shown in Figure 3.

They illustrate the CHL distributions overlaid with Lorenzo's track for four representative days: one pre-hurricane stage (i.e. storm south the area), one during the hurricane, and two post-storm stages (storm north the area). Figure 3 shows that prior to the storm, CHL concentrations along Lorenzo's track were relatively low as expected for this area. Values ranged from a minimum of ~0.05 mg m^{-3} between 20°–30°N in the center of the subtropical gyre, to maximums of 0.1–0.15 mg m^{-3} in both the southern and northern fringes. Following the passage of the hurricane, CHL levels increased across the entire track, up to about 0.15 mg m^{-3} in the subtropical gyre center. By 12 of October (last date in Figure 3), corresponding to 10–15 days after hurricane activity (depending on location), CHL along the track exhibited a decline but remained elevated relative to pre-storm conditions.

The analysis of CHL anomalies (CHLA) was extended up to 12 of October (18 days after the storm first entered the area at 14°N). Figure 4a and 4b displays the distribution and temporal evolution of the daily CHLA relative to the mean CHL concentration averaged over 5 days before hurricane passage, overlaid with Lorenzo's track. The storm induced a positive CHLA along its track, extending over a ~2° band around its trajectory with stronger increases on the right-hand side of Lorenzo's track. The magnitude of the response varied markedly, with several localized peak increases reaching up to 250% north of 20°, and broad enhancements of 100–150% across the whole track. The imagery also indicates that maximum CHL values occur approximately one day after the passage of the hurricane (e.g., Figure 4a, 27–28 September and 1–2 October), after which they decay, although anomalies exceeding 100% persist for up to 10 days or more.

The CHL and CHLA reveal different biological responses to the storm, with patterns varying across ocean regions. To explore the role of different phytoplankton communities, we analyzed PFTs separately by three latitudinal bands (15–25°N, 25–35°N, and 35–40°N). Figure 5 illustrates the distribution over time for the different regions of four major phytoplankton groups: diatoms, haptophytes, dinoflagellates and prokaryotes. Results indicate that all phytoplankton groups increased their concentrations with the passage of Hurricane Lorenzo, though the response varied across regions. While all groups exhibited increases in chlorophyll-a concentration, prokaryotes and haptophytes remained the most dominant groups, consistent with their pre-storm conditions. The strongest response was observed in the 25–35°N region (Figure 5b), where concentrations increased by up to ~50% (e.g., haptophytes from ~0.013 to ~0.02 mg m^{-3}). In the northern 35–40°N region (Figure 5c), however, haptophytes surpassed prokaryotes as the dominant group. Across all regions, concentrations remained elevated for up to at least 10 days relative to pre-storm conditions.

Discussion and conclusions

This study provides insights into the physical and biological responses of the upper ocean to Hurricane Lorenzo, the easternmost Category 5 Atlantic hurricane on record. Using high-resolution daily gap-filled datasets, impacts across different regions of the central North Atlantic were resolved on daily-scales. Results show that Lorenzo induced pronounced SST cooling up to –2.5°C along its track, with the strongest anomalies occurring between 25–37°N (Figure 2). The observed surface cooling is in agreement with previous studies (e.g., Price, 1981 [4]) that link cooling with the TC-induced vertical mixing and the deepening of the mixed layer. The observed asymmetry, with stronger cooling on the right side of the TC track, is a documented phenomenon [4, 5, 30] due to the interaction of storm motion and wind stress curl.

The biological response, measured by CHL (Figure 3) and CHLA (Figure 4), revealed significant chlorophyll enhancement along Lorenzo's path and surrounding areas of ~200 km in diameter. In general, increases of 100-150% were found and positive anomalies persisted for more than 10 days after the storm. These magnitudes are higher when compared to a previous study that examined the impact of 13 hurricanes in the Sargasso Sea, where CHL increases up to a maximum of 91% were documented (Babin et al., 2004 [9]). Importantly, the persistence of elevated CHL levels beyond the immediate post-storm period suggests that TCs can have a lasting influence, at weekly timescales. Furthermore, although localized, we observed CHL increases of up to 250% (Figure 3), which are in line with the fine-scale increases observed by Walker et al., (2005) [10] in Gulf of Mexico. These exacerbated values lasted, on average, 3-4 days at these high levels, as is the case in the area centered at 30°N, 42°W on September 30 (Figure 3a) or at 35°N, 35°W on October 6 (Figure 3b). Interestingly, in both locations Lorenzo was already a Category 2 hurricane, and thus, stronger

CHL anomalies did not coincide with the strongest (Category 4–5) stages of the storm. This supports the notion that wind speed is only one of the factors contributing to changes in CHL. Other factors and pre-storm ocean conditions as likely to play important roles including the depths of the DCM and nitracline, and storm translation speed processes [11].

By incorporating PFT data, we aimed to understand how different phytoplankton groups respond to TC induced perturbations. Examination of the PFT dataset showed that following Hurricane Lorenzo passage all groups increased their concentrations, and Prokaryotes and Haptophytes remained dominant. Only at higher latitudes (35–40°N) there was a change in dominant communities, with Haptophytes surpassing Prokaryotes. The strongest increases (of up to 50%), affecting all phytoplankton groups, occurred in the 25–35°N region (Figure 5b) and are consistent with CHL observations (Figures 3 and 4). These results are in contrast with Avila-Alonso et al. (2023) [19], who highlighted the difficulty of capturing TC-driven biological responses across the subtropical Sargasso Sea using an ecosystem model. This can be explained by differences in methodological approaches and/or the study areas themselves.

The AIGD-PFT dataset allowed to capture daily group specific dynamics, but it remains constrained by model-based assumptions and potential biases in satellite data relationships [31]. Nevertheless, the general dominance of Prokaryotes and Haptophytes (usually dominated by coccolithophores) is consistent with picoplankton (prochlorophytes and cyanobacteria) and prymnesiophytes being important biomass components in subtropical waters [32]. In addition, the Haptophytes dominance shift at midlatitudes could be ascribed to a higher nutrient input in these latitudes following Hurricane Lorenzo, as a result of the northward shallower nutricline. This community shift could be seen as analogue to the seasonal increases in prymnesiophytes biomass following winter mixing and associated nutrient inputs [32]. Overall results suggest that PFTs responded differently to environmental drivers depending on location, and hence that different regional biogeochemistry responses occurred in response to Hurricane Lorenzo.

The results presented here highlight the effect of Hurricane Lorenzo in stimulating chlorophyll. Enhanced surface CHL values, with pronounced peaks 1–2 days after Lorenzo, could be interpreted as the effect of vertical mixing in uplifting of the DCM and/or enhanced growth from the vertical nutrient supply. However, the lagged-response and persistence of high CHL concentrations (>100%) for up to two weeks supports the occurrence of new production, which, in oligotrophic nutrient-limited waters, can only be sustained if nutrients are simultaneously injected into upper levels of the water column and is in line with other studies [9, 11]. It is also worth noting that the magnitude of the CHL response in this study might be of considerable importance when compared with other studies in subtropical North Atlantic, which reported increases only between 5-91% [9]. Despite the present data revealing an ecologically significant, the long-term and annual impact of such events remains uncertain, as TCs are estimated to contribute negligibly to global annual phytoplankton production (~1%, [33]), even though localized increases of 20–30% have been observed [34]. In addition, it is not clear the relative contribution of the increase in chlorophyll in terms of enhanced phytoplankton growth and/or vertical mixing of chlorophyll from the DCM.

Finally, the unusual trajectory of Hurricane Lorenzo demonstrates that latitudes east of 45°W in the Atlantic are also susceptible to grade-5 hurricanes. Although several studies have projected an increase in the severity of these high-impact storms under global warming scenarios [35, 36, 37], it is still unclear how these storms will alter in the future. In this context, understanding the biological response to such extreme events is critical, especially in oligotrophic environments, where a central role in the global carbon cycle is played, contributing more than 30% of global marine carbon fixation [38].

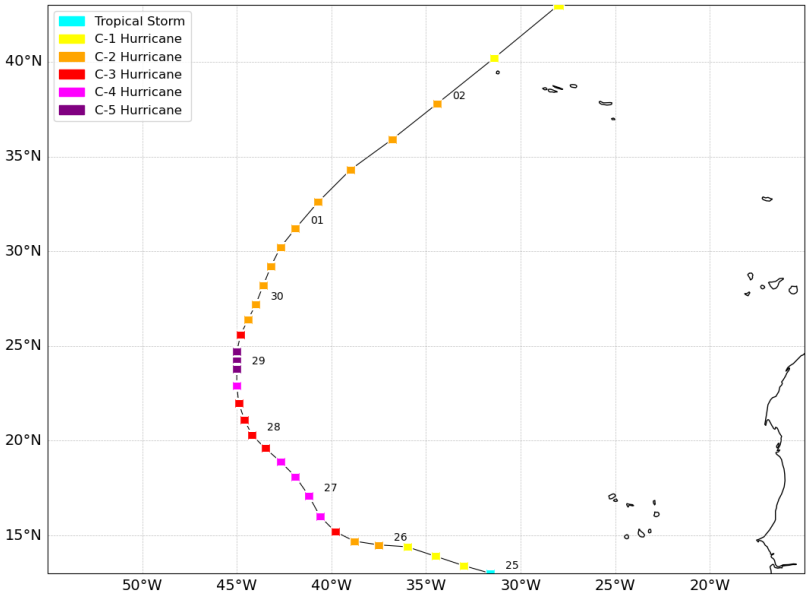

Figure 1. "Best track" positions of Hurricane Lorenzo from 00:00 UTC on 25 September to 12:00 UTC on 2 October 2019. The term "Best Track", as defined by NOAA, refers to the most reliable post analysis estimates of TC track and intensity, derived from a comprehensive assessment of all available data.

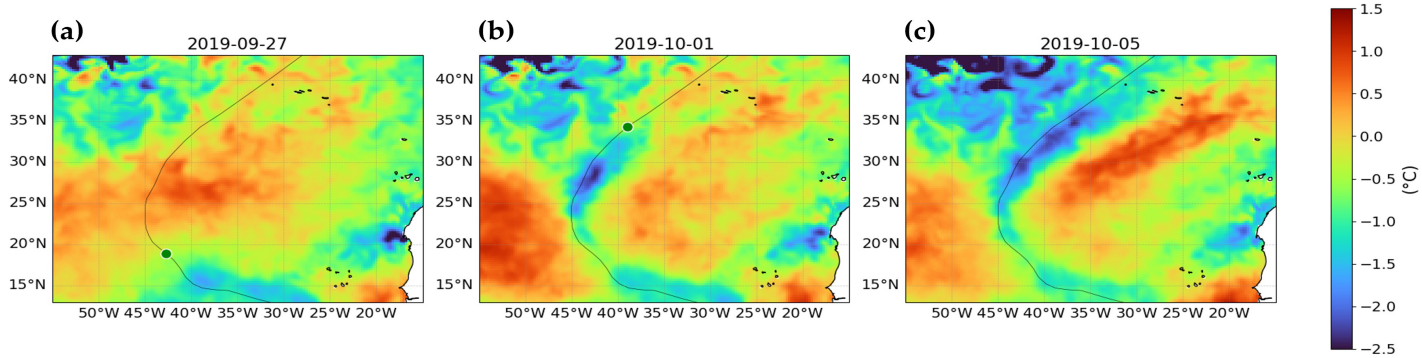

Figure 2. Daily SST anomalies (SSTA) on (**a**) 27 September, (**b**) 1 October and (**c**) 5 October. Anomalies calculated from the Global Ocean OSTIA Sea Surface Temperature and Sea Ice Reprocessed product relative to the 5-day mean prior to Hurricane Lorenzo (17–21 September). The track and position of Hurricane Lorenzo is overlaid.

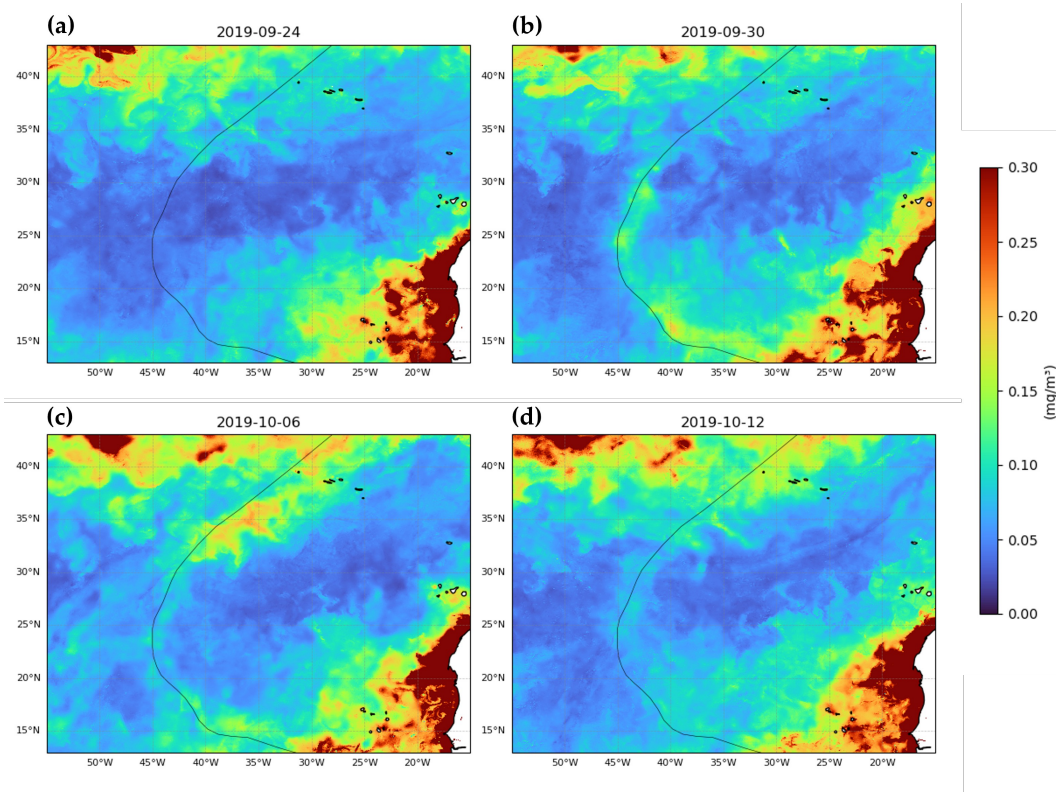

Figure 3. Daily chlorophyll-a concentrations on (a) 24 September, (b) 30 September, (c) 6 October and (d) 12 October. Data from the global multi-sensor Copernicus-GlobColour processor. Lorenzo track and locations are overlaid.

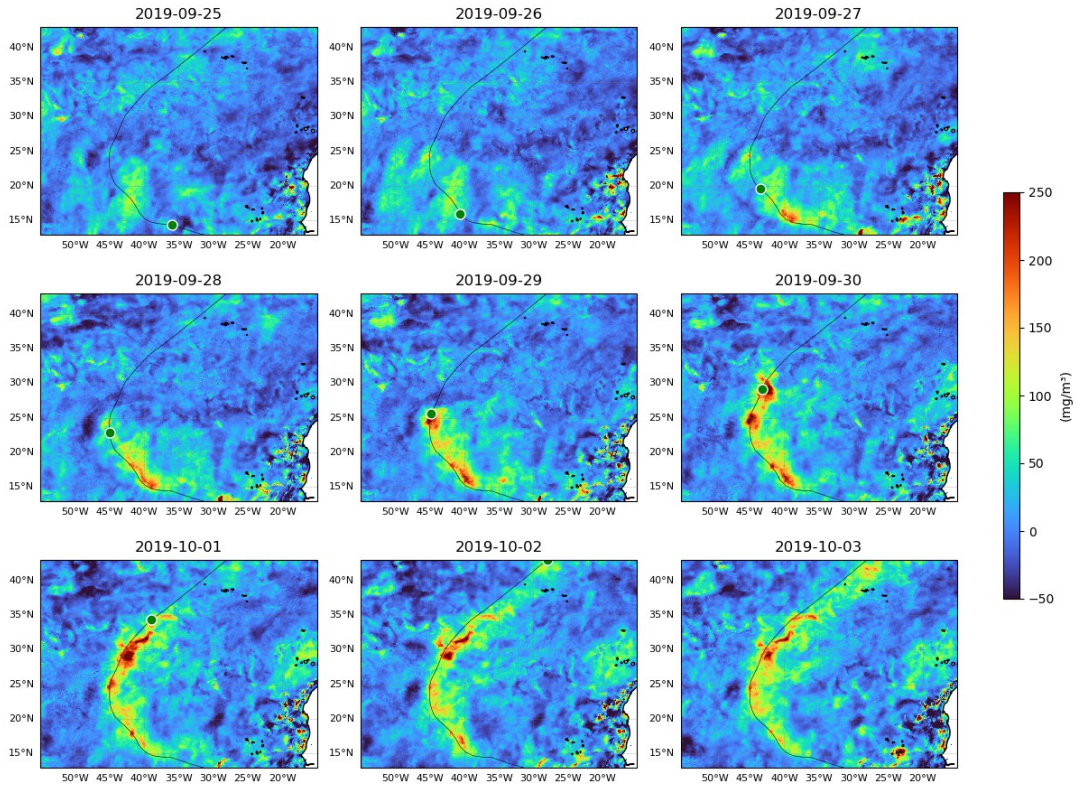

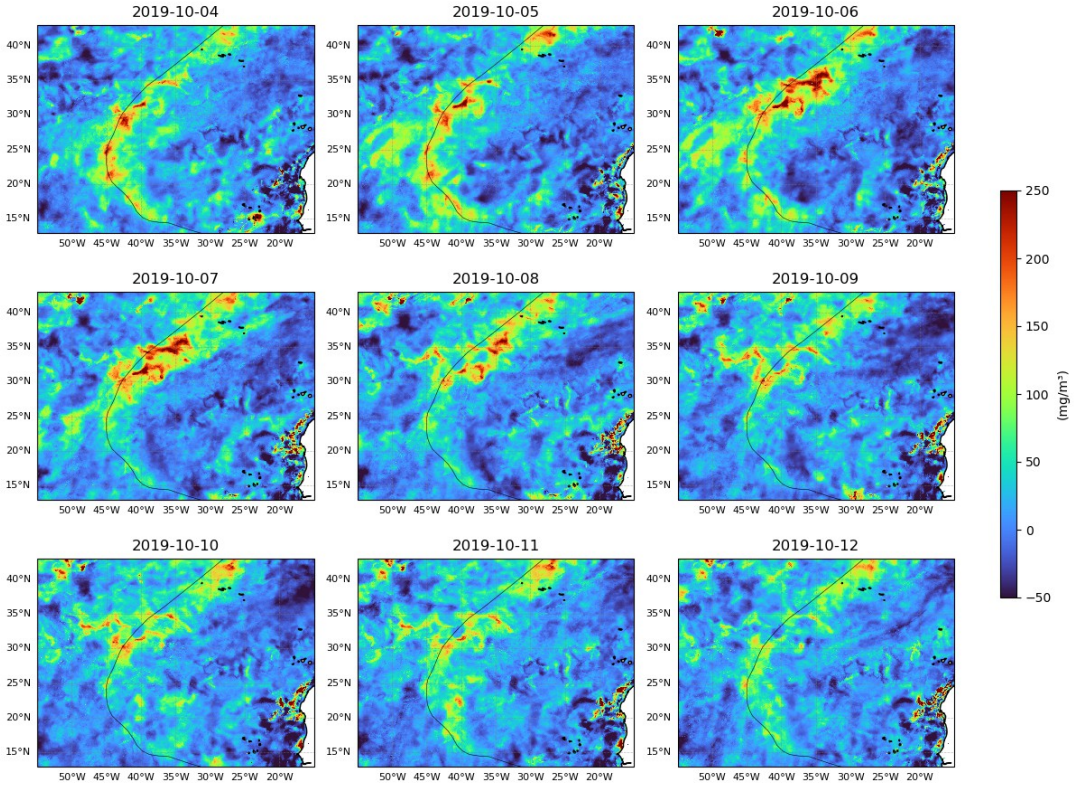

Figure 4. Daily chlorophyll-a anomalies (CHLA) between **(a)** 25 September and 3 October (storm conditions) and **(b)** 4 - 12 October (post-storm conditions). Anomalies calculated from the global multi-sensor Copernicus-GlobColour processor relative to the 5-day mean prior to Hurricane Lorenzo (17–21 September). Lorenzo track and locations are overlaid

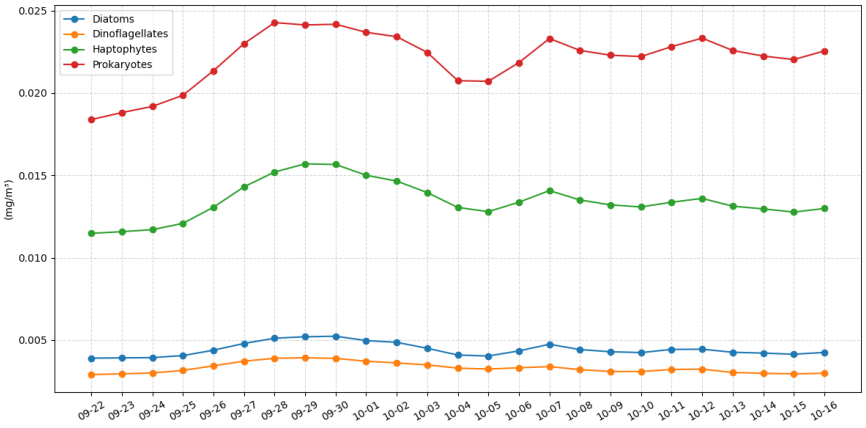

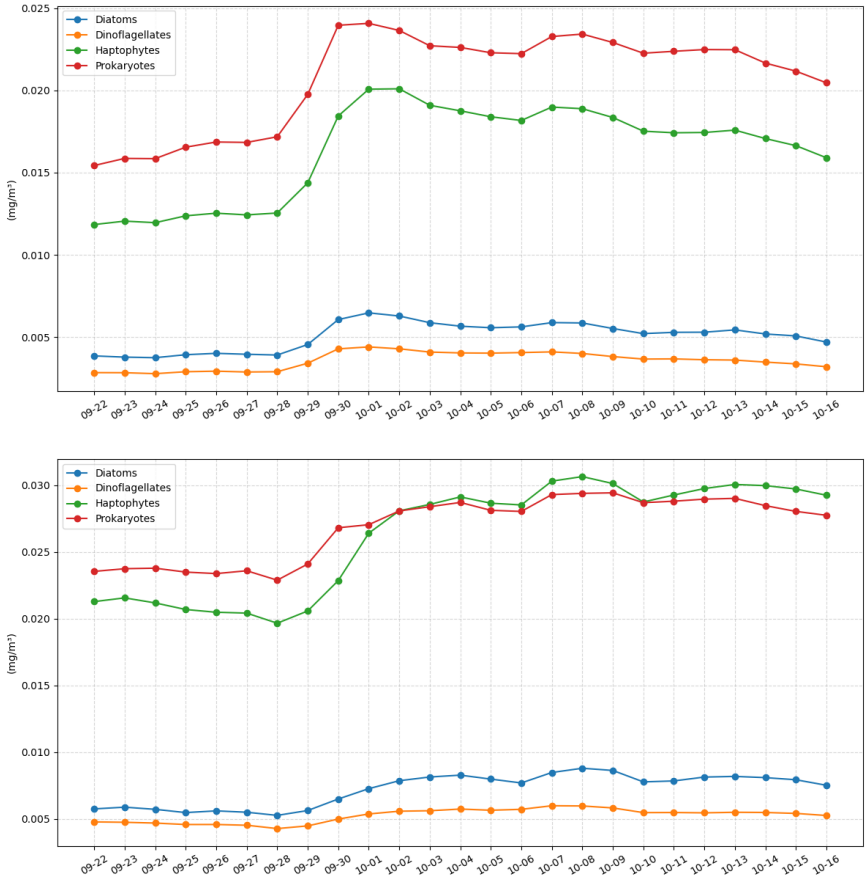

Figure 5. Time series of the major phytoplankton group concentrations, derived from the AIGD-PFT dataset for three regions along Lorenzo's track: **(a)** 15–25°N, **(b)** 25–35°N, and **(c)** 35–40°N. Each series represents regional mean values along the storm track.

References

1. World Meteorological Organization. Global Guide to Tropical Cyclone Forecasting; WMO-No. 1194; WMO: Geneva, Switzerland, 2017.
2. Kouadio, Y.; Machado, L.; Servain, J. Tropical Atlantic Hurricanes, Easterly Waves, and West African Mesoscale Convective Systems. *Advances in Meteorology* **2010**, 284503.
3. Hagen, A.B.; Landsea, C.W. On the Classification of Extreme Atlantic Hurricanes Utilizing Mid-Twentieth-Century Monitoring Capabilities. *J. Climate*, **2012**, *25*, 4461–4475.
4. Price, J.F. Upper Ocean Response to a Hurricane. *Journal of Physical Oceanography* **1981**, *11*, 153–175.
5. Zedler, S.E.; Dickey, T.D.; Doney, S.C.; Price, J.F.; Yu, X.; Mellor, G.L. Analyses and Simulations of the Upper Ocean's Response to Hurricane Felix at the Bermuda Testbed Mooring Site: 13–23 August 1995. *Journal of Geophysical Research: Oceans* **2002**, *107*(C12), 3232.
6. D'Asaro, E.A.; Sanford, T.B.; Niiler, P.P.; Terrill, E.J. Cold Wake of Hurricane Frances. *Geophysical Research Letters* **2007**, *34*, L15609.
7. Price, J.F. Metrics of Hurricane-Ocean Interaction: Vertically-Integrated or Vertically-Averaged Ocean Temperature? *Ocean Science* **2009**, *5*, 351–368.
8. Davis, A.; Yan, X.-H. Hurricane Forcing on Chlorophyll-a Concentration off the Northeast Coast of the U.S. *Geophysical Research Letters* **2004**, *31*, L17304.

9. Babin, S.M.; Carton, J.A.; Dickey, T.D.; Wiggert, J.D. Satellite Evidence of Hurricane-Induced Phytoplankton Blooms in an Oceanic Desert. *Journal of Geophysical Research: Oceans* **2004**, *109*, C03043.
10. Walker, N.D.; Leben, R.R.; Balasubramanian, S. Hurricane-Forced Upwelling and Chlorophyll *a* Enhancement within Cold-Core Cyclones in the Gulf of Mexico. *Geophysical Research Letters* **2005**, *32*, L18610.
11. Shropshire, T.; Li, Y.; He, R. Storm Impact on Sea Surface Temperature and Chlorophyll *a* in the Gulf of Mexico and Sargasso Sea Based on Daily Cloud-Free Satellite Data Reconstructions. *Geophysical Research Letters* **2016**, *43*, 12,199–12,207.
12. Zhao, H.; Wang, Y. Phytoplankton Increases Induced by Tropical Cyclones in the South China Sea during 1998–2015. *Journal of Geophysical Research: Oceans* **2018**, *123*, 2903–2920.
13. Li, Y.; Tang, H. Tropical Cyclone Wind Pump Induced Chlorophyll-a Enhancement in the South China Sea: A Comparison of the Open Sea and Continental Shelf. *Frontiers in Marine Science* **2022**, *9*, 1039824.
14. Falkowski, P.G.; Katz, M.E.; Knoll, A.H.; Quigg, A.; Raven, J.A.; Schofield, O.; Taylor, F.J. The Evolution of Modern Eukaryotic Phytoplankton. *Science* **2004**, *305*(5682), 354–360.
15. Behrenfeld, M.J.; O'Malley, R.T.; Siegel, D.A.; McClain, C.R.; Sarmiento, J.L.; Feldman, G.C.; Milligan, A.J.; Falkowski, P.G.; Letelier, R.M.; Boss, E.S. Climate-Driven Trends in Contemporary Ocean Productivity. *Nature* **2006**, *444*(7120), 752–755.
16. Irwin, A.; Finkel, Z. Mining a Sea of Data: Deducing the Environmental Controls of Ocean Chlorophyll. *PLoS ONE* **2008**, *3*, e3836.
17. Aiken, J.; Alvain, S.; Barlow, R.; Bouman, H.; Bracher, A.; Brewin, B.; Bricaud, A.; Brown, C.; Ciotti, A.; Claustre, H.; Clementson, L.; Craig, S.; Devred, E.; Hirata, T.; Hu, C.; Kostadinov, T.; Lavender, S.; Le Quéré, C.; Uitz, J. Phytoplankton Functional Types from Space. *PLoS ONE* **2014**, *9*, e85747.
18. Mao, Y.; Sun, J.; Guo, C.; Wei, Y.; Wang, X.; Yang, S.; Wu, C. Effects of typhoon Roke and Haitang on phytoplankton community structure in northeastern South China sea. *Ecosystem Health and Sustainability* **2019,** *5*(1), 144–154.
19. Avila-Alonso, D.; Baetens, J.M.; Cardenas, R.; De Baets, B. Response of Phytoplankton Functional Types to Hurricane Fabian (2003) in the Sargasso Sea. *Marine Environmental Research* **2023**, *190*, 106079.
20. Zelinsky, D.A. Hurricane Lorenzo (AL132019). National Hurricane Center Tropical Cyclone Report. **2019**.
21. Campos, R.M.; Bernardino, M.; Gonçalves, M.; Guedes Soares, C. Assessment of Metocean Forecasts for Hurricane Lorenzo in the Azores Archipelago. *Ocean Engineering* **2022**, *243*, 110292.
22. Bahamón, N.; Velásquez, Z.; Cruzado, A. Chlorophyll *a* and Nitrogen Flux in the Tropical North Atlantic Ocean. *Deep Sea Research Part I: Oceanographic Research Papers* **2003**, *50*(10–11), 1189–1203.
23. Signorini, S.R.; Franz, B.A.; McClain, C.R. Chlorophyll Variability in the Oligotrophic Gyres: Mechanisms, Seasonality and Trends. *Frontiers in Marine Science* **2015**, *2*, 1.
24. Lévy, M.; Lehahn, Y.; André, J.-M.; Mémery, L.; Loisel, H.; Heifetz, E. Production Regimes in the Northeast Atlantic: A Study Based on Sea-Viewing Wide Field-of-View Sensor (SeaWiFS) Chlorophyll and Ocean General Circulation Model Mixed Layers. *Journal of Geophysical Research: Oceans* **2005**, *110*, C07S10.
25. Donlon, C.J.; Martin, M.; Stark, J.; Roberts-Jones, J.; Fiedler, E.; Wimmer, W. The Operational Sea Surface Temperature and Sea Ice Analysis (OSTIA) System. *Remote Sensing of Environment* **2012**, *116*, 140–158.
26. Good, S.; Fiedler, E.; Mao, C.; Martin, M.J.; Maycock, A.; Reid, R.; Roberts-Jones, J.; Searle, T.; Waters, J.; While, J.; Worsfold, M. The Current Configuration of the OSTIA System for Operational Production of Foundation Sea Surface Temperature and Ice Concentration Analyses. *Remote Sensing* **2020**, *12*(4), 720.
27. Worsfold, M.; Good, S.; Atkinson, C.; Embury, O. Presenting a Long-Term, Reprocessed Dataset of Global Sea Surface Temperature Produced Using the OSTIA System. *Remote Sensing* **2024**, *16*, 3358.
28. Liu, X.; Wang, M. Global Daily Gap-Free Ocean Color Products from Multi-Satellite Measurements. *International Journal of Applied Earth Observation and Geoinformation* **2022**, *108*, 102714.
29. Ruan, Z.; Hou, X.; Wu, Q.; Li, B.; Wu, Q.; Zou, Y.; et al. Influences of Typhoon Size and Translation Speed on Chlorophyll *a* Response in the Oligotrophic Northwestern Pacific. *Geophysical Research Letters* **2025**, *52*, e2025GL116812.
30. Hanshaw, M.N.; Lozier, M.S.; Palter, J.B. Integrated Impact of Tropical Cyclones on Sea Surface Chlorophyll in the North Atlantic. *Geophysical Research Letters* **2008**, *35*, L01601.
31. Zhang, Y.; Shen, F.; Li, R.; Li, M.; Li, Z.; Chen, S.; Sun, X. AIGD-PFT: The First AI-Driven Global Daily Gap-Free 4 km Phytoplankton Functional Type Data Product from 1998 to 2023. *Earth System Science Data* **2024**, *16*, 4793–4816.

32. Steinberg, D.K.; Carlson, C.A.; Bates, N.R.; Johnson, R.J.; Michaels, A.F.; Knap, A.H. Overview of the US JGOFS Bermuda Atlantic Time-series Study (BATS): a decade-scale look at ocean biology and biogeochemistry. *Deep-Sea Research Part II* **2001**, 48, 1405–1447.
33. Menkes, C.E.; Lengaigne, M.; Lévy, M.; Ethé, C.; Bopp, L.; Aumont, O.; Vincent, E.; Vialard, J.; Jullien, S. Global Impact of Tropical Cyclones on Primary Production. *Global Biogeochemical Cycles* **2016**, *30*, 767–786.
34. Lin, I.; Liu, W.T.; Wu, C.-C.; Wong, G.T.F.; Hu, C.; Chen, Z.; Liang, W.-D.; Yang, Y.; Liu, K.-K. New Evidence for Enhanced Ocean Primary Production Triggered by Tropical Cyclone. *Geophysical Research Letters* **2003**, *30*(13), 1718.
35. Emanuel, K. Increasing Destructiveness of Tropical Cyclones over the Past 30 Years. *Nature* **2005**, *436*, 686–688. https://doi.org/10.1038/nature03906
36. Knutson, T.; et al. Tropical Cyclones and Climate Change Assessment: Part II: Projected Response to Anthropogenic Warming. *Bulletin of the American Meteorological Society* **2020**, *101*, E303–E322.
37. Pérez-Alarcón, A.; Coll-Hidalgo, P.; Fernández-Alvarez, J.C.; Trigo, R.M.; Nieto, R.; Gimeno, L. Evaluating Changes in the Moisture Sources for Tropical Cyclones Precipitation in the North Atlantic That Underwent Extratropical Transition. *Geophysical Research Letters* **2023**, *50*, e2022GL102120.
38. Longhurst, A.; Sathyendranath, S.; Platt, T.; Caverhill, C. An Estimate of Global Primary Production in the Ocean from Satellite Radiometer Data. *Journal of Plankton Research* **1995**, *17*(6), 1245–1271.